A microscopic study of strongly plasmonic Au and Ag island thin films

Prathamesh Pavaskar, I-Kai Hsu, Jesse Theiss, Wei Hsuan Hung, and Stephen B. Cronin

Related Articles

Additional information on J. Appl. Phys.

A microscopic study of strongly plasmonic Au and Ag island thin films

Prathamesh Pavaskar,[1] I-Kai Hsu,[2] Jesse Theiss,[1] Wei Hsuan Hung,[3] and Stephen B. Cronin[1,a)]

[1]Department of Electrical Engineering, University of Southern California, Los Angeles, California 90089, USA
[2]Department of Materials Science, University of Southern California, Los Angeles, California 90089, USA
[3]Department of Materials Science and Engineering, Feng Chia University, Taichung 407, Taiwan

Thin Au and Ag evaporated films ($\sim$5 nm) are known to form island-like growth, which exhibit a strong plasmonic response under visible illumination. In this work, evaporated thin films are imaged with high resolution transmission electron microscopy, to reveal the structure of the semicontinuous metal island film with sub-nm resolution. The electric field distributions and the absorption spectra of these semicontinuous island film geometries are then simulated numerically using the finite difference time domain method and compared with the experimentally measured absorption spectra. We find surface enhanced Raman scattering (SERS) enhancement factors as high as 10^8 in the regions of small gaps (≤ 2 nm), which dominate the electromagnetic response of these films. The small gap enhancement is further substantiated by a statistical analysis of the electric field intensity as a function of the nanogap size. Areal SERS enhancement factors of 4.2×10^4 are obtained for these films. These plasmonic films can also enhance the performance of photocatalytic and photovoltaic phenomena, through near-field coupling. For TiO_2 photocatalysis, we calculate enhancement factors of 16 and 19 for Au and Ag, respectively. We study the effect of annealing on these films, which results in a large reduction in electric field strength due to increased nanoparticle spacing. © 2013 American Institute of Physics.
[http://dx.doi.org/10.1063/1.4775784]

INTRODUCTION

Plasmonic phenomena have demonstrated great promise for a variety of photonic device applications including sub-wavelength waveguides,[1] tunable filters,[2] resonators,[3] and modulators.[4] Plasmonic lasers,[5,6] photocatalysts,[7–10] and solar cells[11–14] have also been realized experimentally. A wide range of fabrication techniques exist for producing plasmonic nanostructures including electron beam lithography,[15] colloidal self assembly,[16,17] nanoimprint lithography,[18] nanosphere lithography,[19,20] and block copolymer lithography,[21] just to name a few. Thin films ($\sim$5 nm) of noble metals evaporated on dielectric substrates present a simple one-step and reproducible way to make stable plasmonic nanostructures. These semicontinuous thin films of Ag or Au have been used in surface enhanced Raman scattering (SERS),[22,23] plasmon-enhanced photocatalysis,[7–9] and sensing applications.[24–26] SERS enhancement factors of 10^5 have been previously reported for Ag films.[27] Van Duyne et al. showed that large electric field enhancements are obtained due to the island-like structure of these films.[27] Regions of strong local electric field enhancements called "hot spots" are observed between the nanoislands.[28] An extensive study of these thin films has been done by the Purdue group both theoretically[28–30] and experimentally.[31,32] These hot spots are generally believed to be formed in regions in which the gaps between neighboring islands are very small, which allows for maximum plasmonic coupling.

This is a well-known plasmonic phenomenon in the case of nanoparticle dimers.[15,33–35] While these semicontinuous films consist of random geometries of metal islands, their performance is significant and reproducible. We would like to develop an understanding of the microscopic electric field distribution of these substrates, and their relationship to nanoparticle morphology.

In previous works, the morphology of these semicontinuous metal island films have been studied by scanning electron microscopy (SEM),[36,37] transmission electron microscopy (TEM),[38] scanning tunneling microscopy (STM),[39] and atomic force microscopy (AFM).[27,40] Schlegel and Cotton,[38] using TEM, and Dawson et al.,[39] using STM, studied the relationship of the deposition rate of silver films with SERS intensities. Both these works showed that slowly deposited films produce higher SERS intensities than rapidly deposited films. Electromagnetic simulations of semicontinuous metal films have been carried out based on SEM and AFM images by several groups.[27,30,40,41] In the work presented here, finite difference time domain method (FDTD) simulations are performed based on HRTEM images, which provide a spatial resolution more than one order of magnitude higher than previous studies. The grid size of the FDTD calculations are also one order of magnitude higher than previous studies, which is important in accurately capturing the behavior of the quickly decaying fields at the surface of these metals.

EXPERIMENTAL AND SIMULATION DETAILS

Electron-beam evaporation was used to deposit 5 nm and 10 nm Au and Ag films on 100 nm thick SiN membranes,

a)Electronic mail: scronin@usc.edu.

as determined by a quartz crystal oscillator thickness monitor. A JEOL JEM-2100F advanced field emission transmission electron microscope was used to obtain high resolution TEM images of these films with a resolution of <2 Å. FDTD simulations were performed on USC's 0.15 petaflop supercomputing facility, which consists of 14 734 CPUs connected by a high-performance, low-latency Myrinet network. For the simulations, a cell of size 1000 nm × 800 nm × 500 nm is used, which represents an experimentally measurable area, larger than the diffraction limit. The film occupies an area of 450 nm × 300 nm in the simulation. We use a grid spacing of 2 Å in the volume of 500 nm × 500 nm × 40 nm around the film and 10 nm elsewhere. A temporal grid spacing of 0.002 fs is used with a total of 100 000 time steps. A planewave source is used, which irradiates the metal film with a Gaussian pulse with a spectrum of wavelengths ranging from 300 nm to 800 nm. Perfectly matched layers (PML) boundary conditions are used with 25 layers. The dielectric functions of Au and Ag are based on the optical constants given by Palik and Ghosh.[42]

RESULTS AND DISCUSSION

Figures 1(a), 1(c), and 1(e) show high resolution TEM images of Au and Ag thin films with nominal thicknesses of 5 nm and 10 nm. The island-like formations are clearly
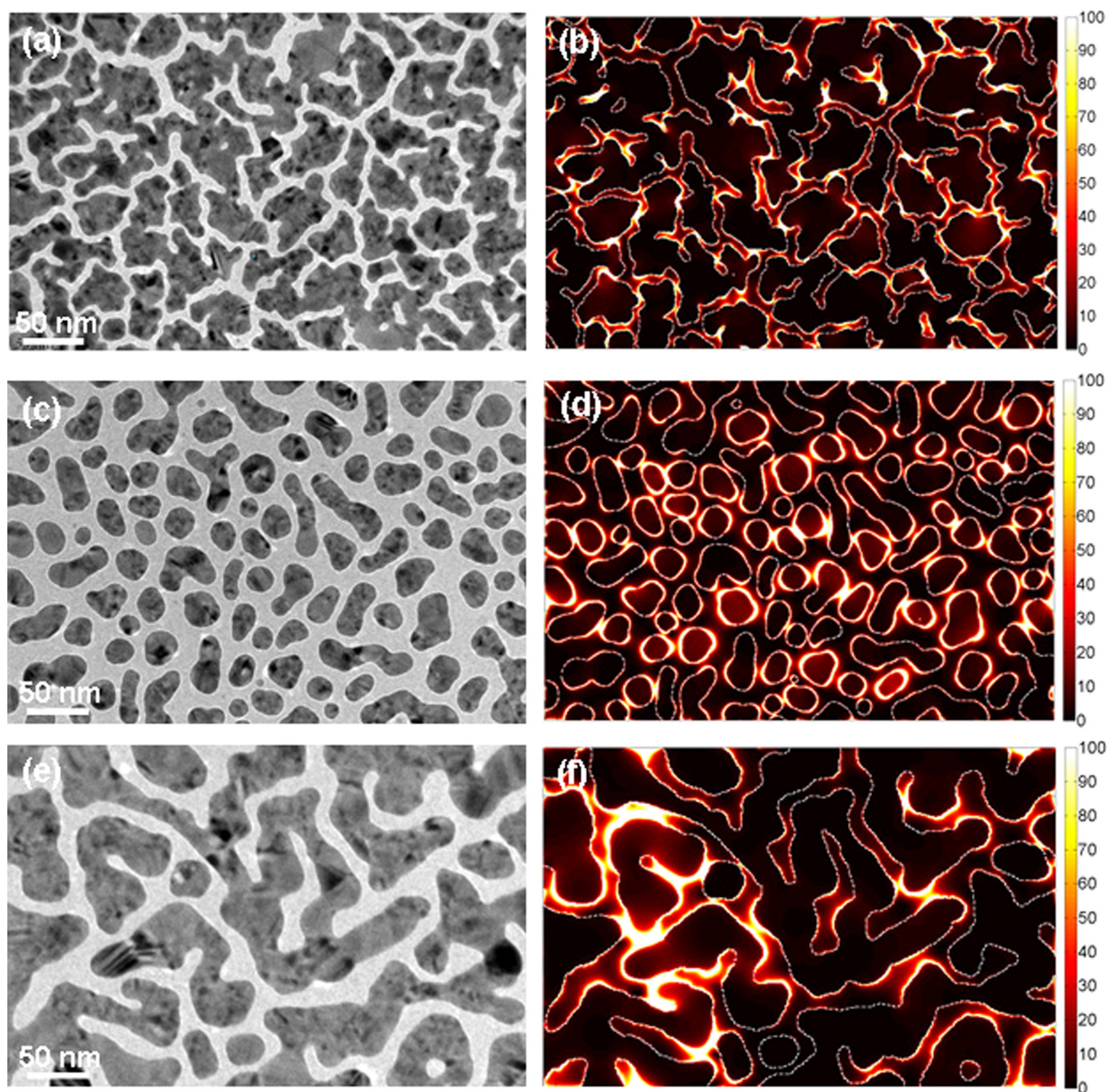

FIG. 1. TEM images and electric field profiles of (a) and (b) a 5 nm thick Au island film, (c) and (d) a 5 nm thick Ag film, and (e) and (f) a 10 nm thick Ag film. The color axes in (b), (d), and (f) show the enhancement of electric field intensity relative to the incident electric field intensity.

visible in the images, where the dark grey regions are the gold or silver islands and the light grey regions are interstitial space in between. The 5 nm Ag island nanoparticles (Figure 1(c)) are more loosely packed than the Au island film (Figure 1(a)) because the percolation threshold (i.e., the thickness above which the film goes from being insulating to conductive) for Ag films is 10 nm.[43,44] Figure 1(e) shows the TEM image of a 10 nm thick Ag film. Figures 1(b), 1(d), and 1(f) show the electric field distribution of the Au and Ag films. Here, the color axes show the enhancement of electric field intensity relative to the incident electric field intensity. The Au film shows higher electric field intensities than Ag, due to the smaller gaps between the islands. As postulated before, these results show that SERS enhancement is dominated by a few nm-sized hot spots rather than regions extending over large areas. As such, these films utilize only a very small fraction of the sample area. For the gold film, the local electric field intensity in each of these hot spot regions is approximately three to four orders of magnitude larger than the incident electric field.

Figure 2 shows the calculated and measured absorption spectra of the Au and Ag films shown in Figure 1. The experimental absorption spectra were measured using a Perkin-Elmer Lambda 950 UV/Vis/NIR spectrometer with an integrating sphere detector. These figures show good agreement between the experimental and calculated spectra, which confirms the accuracy of our simulations. The absorption spectra for the 5 nm Au film and 10 nm Ag film show a much broader response than the 5 nm Ag film, due to the inhomogeneity of the island shapes and sizes, which gives rise to different plasmon modes.[45]

Figures 3(a) and 3(b) show the polarization dependence of the electromagnetic response of the 5 nm Au film. As can be seen in these figures, gaps oriented vertically are primarily excited by horizontally polarized light and vice versa. This polarization dependence confirms the notion that the hot spots are formed due to strong plasmonic coupling between nearly touching islands. Some of the hot spots can produce SERS intensity enhancements exceeding 10^8. The average electric field intensity enhancements for various gap sizes is shown in Figure 3(c), where each data point is a statistical average of several hot spots of the same gap size. There is a monotonic decrease in the enhancement by a factor of 117, as the gap size increases from 2 nm to 10 nm, further demonstrating that the high electric fields in the gaps are due to strong plasmonic coupling. Such a relation between the electric field and the gap size has been shown previously in the case of dimers[34,46] but not in the case of island films. It should be noted that sub-10 nm gaps cannot be fabricated by standard lithographic techniques.

We have also investigated the effect of annealing on nanoparticle morphology and the absorption spectra of these films. Figure 4(a) shows a high resolution TEM image of a 5 nm Au film after annealing at 200 °C for 2 h. The absorption spectra taken of annealed Au and Ag films are shown Figures 4(b) and 4(c). These spectra exhibit narrow plasmon resonant absorption centered at 540 nm and 474 nm for Au and Ag, respectively, which is consistent with the absorption
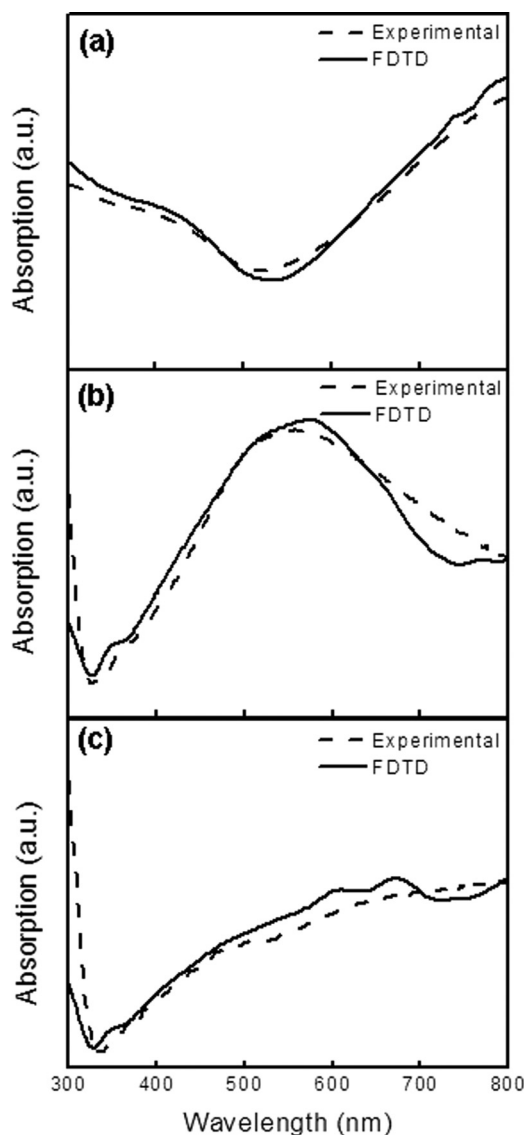

FIG. 2. Experimental and simulated absorption spectra of (a) 5 nm Au, (b) 5 nm Ag, and (c) 10 nm Ag island films.

spectra of isolated nanoparticles. This occurs due to the fact that this random distribution of island shapes is transformed into a fairly uniform distribution of ellipsoidal nanoparticles after annealing.

From the FDTD simulations described above, we have calculated the SERS enhancement factors of these films. Since the Raman intensity depends on the electric field to the fourth power (E^4), for small phonon energies, each of the hot spot regions is able to produce a SERS enhancement factors exceeding 10^8. However, this requires that the molecule(s) of interest be located precisely in the 1–2 nm hot spot region. Therefore, most of the area of this film does not demonstrate significant SERS enhancement. This makes detecting trace amounts of chemical species difficult and impractical. The areal SERS enhancement is another way to assess the performance of SERS substrates and is obtained by integrating E^4 over the entire sample area and dividing by the incident electric field to the fourth power (E_o^4) integrated over the same area, as follows:
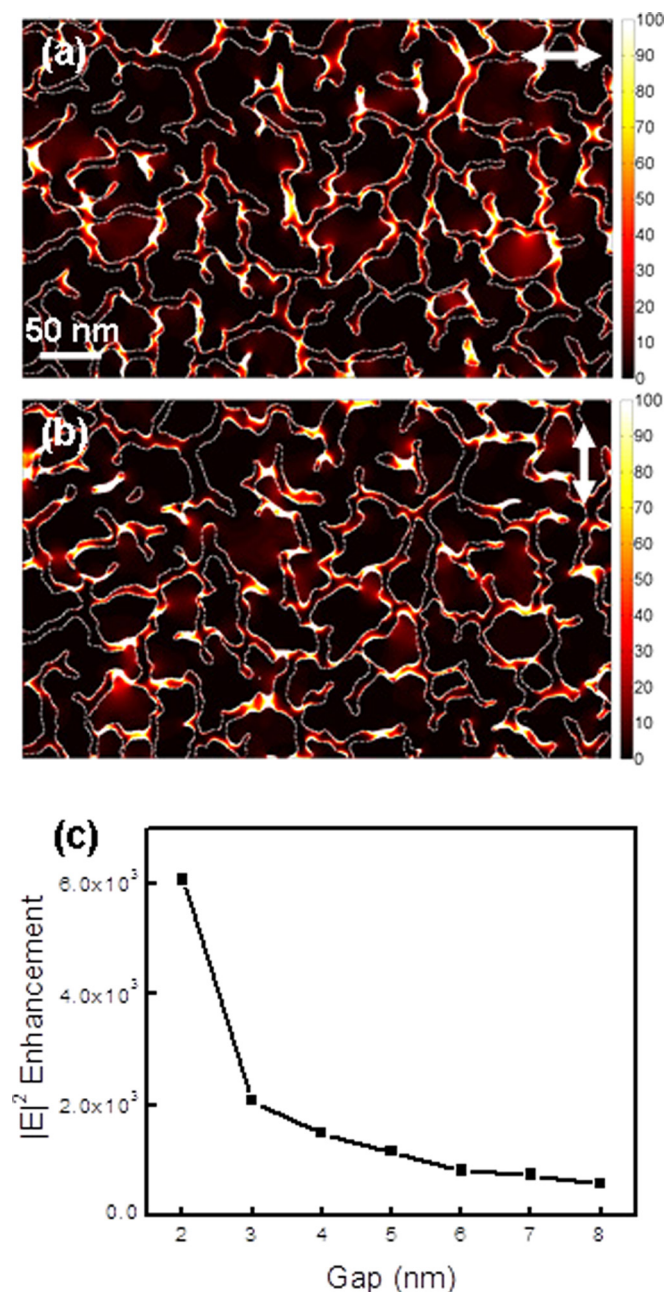
FIG. 3. Electric field distribution of a 5 nm Au film irradiated with (a) horizontally and (b) vertically polarized light. (c) The distribution of the electric field intensity enhancements for various gap sizes. The color axes in (a) and (b) show the enhancement of electric field intensity relative to the incident electric field intensity.

$$\text{Areal SERS enhancement factor} = \frac{\int dxdy |E|^4}{\int dxdy |E_0|^4}. \quad (1)$$

Based on this equation, an areal SERS enhancement factor of 4.2×10^4 was obtained for both the 5 nm Au and 10 nm Ag films. The 5 nm Ag film exhibited a smaller enhancement of 1.3×10^4 because the islands are more loosely packed resulting in a fewer number of small nanogaps. The annealed films produced even smaller enhancement factors of 366 and 45 for the Au and Ag films, respectively. Another reason for the smaller enhancements of the 5 nm Ag film and the annealed Au and Ag films is their lack of pointed and sharp
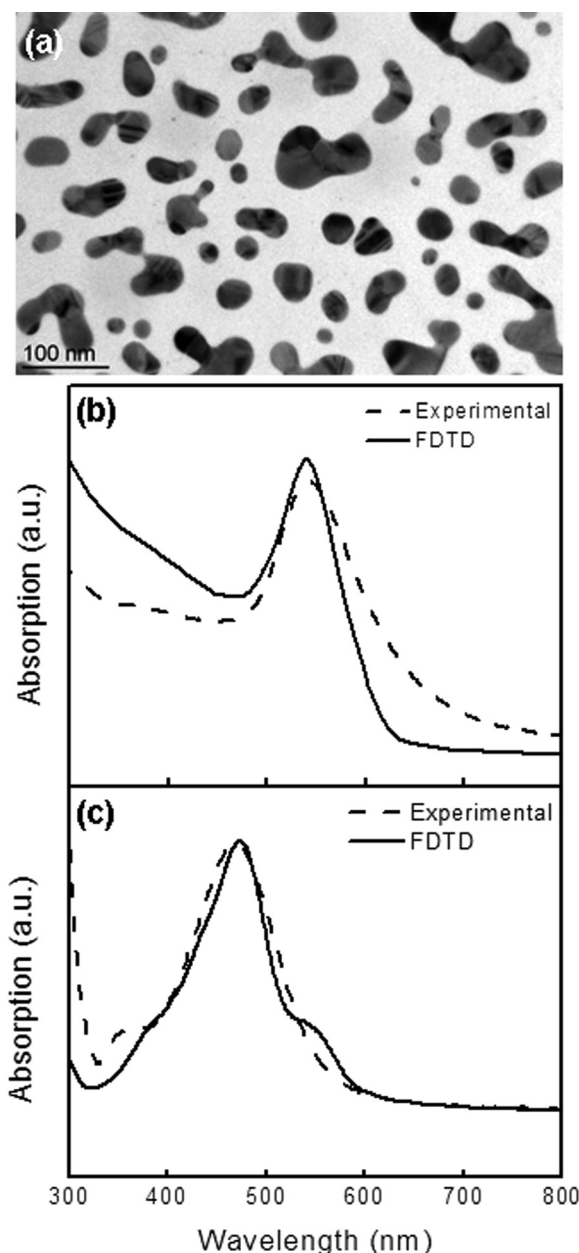

FIG. 4. (a) TEM image of an annealed 5 nm Au film. Experimental and simulated absorption spectra of annealed 5 nm (b) Au and (c) Ag films.

edges. It has been shown previously that such sharp features give rise to large plasmonic enhancements due to the so called lightning rod effect.[47–49]

In addition to SERS enhancement, we have also calculated the photocatalytic enhancement factors for these plasmonic metal island films, as reported previously for nanoparticles deposited on top of a photocatalytic semiconductor. For the photocatalytic enhancement factor, we integrate over E^2 instead of E^4, since the electron-hole pair generation rate is proportional to the square of the electric field. For the calculation of the photocatalytic enhancement factor, we need to consider absorption in the underlying substrate, since the electron-hole pairs driving the photocatalytic reaction are created in the substrate. Therefore, we also integrate over the z-dimension in our calculation. Since the minority carrier

diffusion length in TiO_2 is only about $10\,nm$, we only integrate over that length in the z-direction. Thus, the formula for the photocatalytic enhancement factor is

$$\text{Photocatalytic enhancement factor} = \frac{\int_{-10nm}^{0} dz \int dxdy |E|^2}{\int_{-10nm}^{0} dz \int dxdy |E_{sub}|^2}, \tag{2}$$

where E_{sub} is the electric field intensity in the underlying semiconductor without the plasmonic film. The dielectric function of anatase TiO_2 is used for the substrate.[50] Using this formula, the calculated photocatalytic enhancement factors for $5\,nm$ Au and $10\,nm$ Ag films are 16 and 19, respectively. For a single hot spot, this enhancement factor is 176 in the $5\,nm$ Au film. The annealed films barely produce any enhancement with photocatalytic enhancement factors of 2.8 and 2.2 for the Au and Ag films, respectively.

Several experimental photocatalytic studies have reported plasmonic enhancement using these $5\,nm$ semi-continuous Au films deposited on top of photocatalytic semiconductors. For water splitting, photocatalytic enhancement factors of 4 and 66 were reported at $532\,nm$ and $633\,nm$, respectively.[9] For methane formation from the reduction of CO_2 with water, a plasmonic enhancement factor of $24\times$ was reported.[7] While these experimental values span a wide range, the enhancement is of the same order of magnitude as that predicted from the electric field distributions of FDTD simulations for similar nano-island films conducted in this study.

CONCLUSIONS

In conclusion, we have simulated semicontinuous thin films of Au and Ag based on high resolution transmission electron microscope images with $2\,\mathring{A}$ resolution using the finite difference time domain method. The island-like structure of these films produces strongly plasmonic behavior due to the presence of "hot spots" located between small nm-sized gaps. Our results verify the notion previously put forth that macroscopically observed SERS is dominated by a few nm-sized "hot spots," with SERS intensities reaching 10^8 times the incident intensity. We obtained photocatalytic enhancement factors of 16 and 19 for $5\,nm$ Au and $10\,nm$ Ag films, respectively, over the whole film, but a much higher enhancement factor of 176 for a single hot spot. This indicates that if these films are optimized to have a large number of hot spots using numerical optimization, much higher enhancement factors over the whole film can be obtained. Based on a statistical analysis of electric field enhancements for various gap sizes, we demonstrate that the hot spots arise due to strong plasmonic coupling between nearly touching islands. Thermal annealing of these island films results in significant changes in their morphology and absorption spectra.

ACKNOWLEDGMENT

[1]S. A. Maier, P. G. Kik, H. A. Atwater, S. Meltzer, E. Harel, B. E. Koel, and A. A. G. Requicha, Nature Mater. **2**, 229 (2003).

[2]K. Diest, J. A. Dionne, M. Spain, and H. A. Atwater, Nano Lett. **9**, 2579 (2009).

[3]I. Bulu, T. Babinec, B. Hausmann, J. T. Choy, and M. Loncar, Opt. Express **19**, 5268 (2011).

[4]J. A. Dionne, K. Diest, L. A. Sweatlock, and H. A. Atwater, Nano Lett. **9**, 897 (2009).

[5]R. F. Oulton, V. J. Sorger, T. Zentgraf, R. M. Ma, C. Gladden, L. Dai, G. Bartal, and X. Zhang, Nature **461**, 629 (2009).

[6]E. Cubukcu, E. A. Kort, K. B. Crozier, and F. Capasso, Appl. Phys. Lett. **89**, 093120 (2006).

[7]W. Hou, W. H. Hung, P. Pavaskar, A. Goeppert, M. Aykol, and S. B. Cronin, ACS Catal. **1**, 929 (2011).

[8]W. Hou, Z. Liu, P. Pavaskar, W. H. Hung, and S. B. Cronin, J. Catal. **277**, 149 (2011).

[9]Z. Liu, W. Hou, P. Pavaskar, M. Aykol, and S. B. Cronin, Nano Lett. **11**, 1111 (2011).

[10]I. Thomann, B. Pinaud, Z. Chen, B. Clemens, T. Jaramilo, and M. L. Brongersma, Nano Lett. **11**, 3440 (2011).

[11]K. Nakayama, K. Tanabe, and H. A. Atwater, Appl. Phys. Lett. **93**, 121904 (2008).

[12]H. A. Atwater and A. Polman, Nature Mater. **9**, 205 (2010).

[13]V. E. Ferry, L. A. Sweatlock, D. Pacifici, and H. A. Atwater, Nano Lett. **8**, 4391 (2008).

[14]W. Hou, P. Pavaskar, Z. Liu, J. Theiss, M. Aykol, and S. B. Cronin, Energy Environ. Sci. **4**, 4650 (2011).

[15]J. Theiss, P. Pavaskar, P. M. Echternach, R. E. Muller, and S. B. Cronin, Nano Lett. **10**, 2749 (2010).

[16]J. J. Storhoff, A. A. Lazarides, R. C. Mucic, C. A. Mirkin, R. L. Letsinger, and G. C. Schatz, J. Am. Chem. Soc. **122**, 4640 (2000).

[17]A. A. Lazarides and G. C. Schatz, J. Phys. Chem. B **104**, 460 (2000).

[18]W. Wu, Z. Yu, S. Y. Wang, R. S. Williams, Y. Liu, C. Sun, X. Zhang, E. Kim, Y. R. Shen, and N. X. Fang, Appl. Phys. Lett. **90**, 063107 (2007).

[19]C. L. Haynes and R. P. Van Duyne, J. Phys. Chem. B **105**, 5599 (2001).

[20]K. Chen, C. Durak, J. R. Heflin, and H. D. Robinson, Nano Lett. **7**, 254 (2007).

[21]T. F. Jaramillo, S. H. Baeck, B. R. Cuenya, and E. W. McFarland, J. Am. Chem. Soc. **125**, 7148 (2003).

[22]K. Kneipp, H. Kneipp, P. Corio, S. D. M. Brown, K. Shafer, J. Motz, L. T. Perelman, E. B. Hanlon, A. Marucci, G. Dresselhaus, and M. S. Dresselhaus, Phys. Rev. Lett. **84**, 3470 (2000).

[23]P. Corio, S. D. M. Brown, A. Marucci, M. A. Pimenta, K. Kneipp, G. Dresselhaus, and M. S. Dresselhaus, Phys. Rev. B **61**, 13202 (2000).

[24]G. Kalyuzhny, A. Vaskevich, G. Ashkenasy, A. Shanzer, and I. Rubinstein, J. Phys. Chem. B **104**, 8238 (2000).

[25]G. Kalyuzhny, A. Vaskevich, M. A. Schneeweiss, and I. Rubinstein, Chem.-Eur. J. **8**, 3849 (2002).

[26]I. Tokareva, S. Minko, J. H. Fendler, and E. Hutter, J. Am. Chem. Soc. **126**, 15950 (2004).

[27]R. P. Van Duyne, J. C. Hulteen, and D. A. Treichel, J. Chem. Phys. **99**, 2101 (1993).

[28]F. Brouers, S. Blacher, A. N. Lagarkov, A. K. Sarychev, P. Gadenne, and V. M. Shalaev, Phys. Rev. B **55**, 13234 (1997).

[29]F. Brouers, S. Blacher, and A. K. Sarychev, Phys. Rev. B **58**, 15897 (1998).

[30]U. K. Chettiar, P. Nyga, M. D. Thoreson, A. V. Kildishev, V. P. Drachev, and V. M. Shalaev, Appl. Phys. B: Lasers Opt. **100**, 159 (2010).

[31]S. Gresillon, L. Aigouy, A. C. Boccara, J. C. Rivoal, X. Quelin, C. Desmarest, P. Gadenne, V. A. Shubin, A. K. Sarychev, and V. M. Shalaev, Phys. Rev. Lett. **82**, 4520 (1999).

[32]S. Ducourtieux, V. A. Podolskiy, S. Grésillon, S. Buil, B. Berini, P. Gadenne, A. C. Boccara, J. C. Rivoal, W. D. Bragg, and K. Banerjee, Phys. Rev. B **64**, 165403 (2001).

[33]C. Oubre and P. Nordlander, J. Phys. Chem. B **109**, 10042 (2005).

[34]E. Hao and G. C. Schatz, J. Chem. Phys. **120**, 357 (2004).

[35]S. Palomba, M. Danckwerts, and L. Novotny, J. Opt. A, Pure Appl. Opt. **11**, 114030 (2009).

[36]P. Royer, J. P. Goudonnet, R. J. Warmack, and T. L. Ferrell, Phys. Rev. B **35**, 3753 (1987).

[37]R. Kumar, H. Zhou, and S. B. Cronin, Appl. Phys. Lett. **91**, 223105 (2007).

[38]V. Schlegel and T. Cotton, Anal. Chem. **63**, 241 (1991).

[39]P. Dawson, K. Alexander, J. Thompson, J. Haas III, and T. Ferrell, Phys. Rev. B **44**, 6372 (1991).

[40]S. Buil, J. Laverdant, B. Berini, P. Maso, J. P. Hermier, and X. Quélin, Opt. Express **20**, 11968 (2012).

[41]G. C. Schatz, Acc. Chem. Res. **17**, 370 (1984).

[42]E. D. Palik and G. Ghosh, *Handbook of Optical Constants of Solids* (Academic, 1998), Vol. 3.

[43]M. D. Thoreson, J. Fang, A. V. Kildishev, L. J. Prokopeva, P. Nyga, U. K. Chettiar, V. M. Shalaev, and V. P. Drachev, J. Nanophotonics **5**, 051513 (2011).

[44]A. L. Efros and B. I. Shklovskii, Phys. Status Solidi B **76**, 475 (1976).

[45]D. A. Genov, A. K. Sarychev, and V. M. Shalaev, J. Nonlinear Opt. Phys. Mater. **12**, 419 (2003).

[46]J. Aizpurua, G. W. Bryant, L. J. Richter, F. J. G. De Abajo, B. K. Kelley, and T. Mallouk, Phys. Rev. B **71**, 235420 (2005).

[47]S. A. Maier and H. A. Atwater, J. Appl. Phys. **98**, 011101 (2005).

[48]J. I. Gersten, J. Chem. Phys. **72**, 5779 (1980).

[49]M. I. Stockman, Phys. Rev. Lett. **93**, 137404 (2004).

[50]S. D. Mo and W. Y. Ching, Phys. Rev. B **51**, 13023 (1995).